

## Clodronate-Liposome Mediated Macrophage Depletion Abrogates Multiple Myeloma Tumor Establishment *In Vivo*



Khatora S. Opperman<sup>\*,†</sup>, Kate Vandyke<sup>\*,†</sup>, Kimberley C. Clark<sup>\*,†</sup>, Elizabeth A. Coulter<sup>\*,†</sup>, Duncan R. Hewett<sup>\*,†</sup>, Krzysztof M. Mrozik<sup>\*,†</sup>, Nisha Schwarz<sup>‡</sup>, Andreas Evdokiou<sup>§,¶</sup>, Peter I Croucher<sup>#</sup>, Peter J Psaltis<sup>‡</sup>, Jacqueline E Noll<sup>\*,†,1</sup> and Andrew CW Zannettino<sup>\*,†,\*\*,1</sup>

<sup>\*</sup>Myeloma Research Laboratory, Adelaide Medical School, Faculty of Health and Medical Sciences, University of Adelaide, North Terrace, Adelaide, 5005; <sup>†</sup>Cancer Program, Precision Medicine Theme, South Australian Health and Medical Research Institute, PO Box 11060, Adelaide, 5001; <sup>‡</sup>Heart and Vascular Health Program, Lifelong Health Theme, South Australian Health and Medical Research Institute, PO Box 11060, Adelaide, 5001; <sup>§</sup>Discipline of Surgery, Adelaide Medical School, Faculty of Health and Medical Sciences, University of Adelaide, North Terrace, Adelaide, 5005; <sup>¶</sup>Basil Hetzel Institute, 37 Woodville Road, Woodville, 5011; <sup>#</sup>Bone Biology Laboratory, Garvan Institute of Medical Research, 384 Victoria Street, Darlinghurst, NSW, 2010; <sup>\*\*</sup>Centre for Cancer Biology, University of South Australia and SA Pathology, PO Box 2471, Adelaide, 5001

### Abstract

Multiple myeloma is a fatal plasma cell malignancy that is reliant on the bone marrow microenvironment. The bone marrow is comprised of numerous cells of mesenchymal and hemopoietic origin. Of these, macrophages have been implicated to play a role in myeloma disease progression, angiogenesis, and drug resistance; however, the role of macrophages in myeloma disease establishment remains unknown. In this study, the antimyeloma efficacy of clodronate-liposome treatment, which globally and transiently depletes macrophages, was evaluated in the well-established C57BL/KaLwRijHsd murine model of myeloma. Our studies show, for the first time, that clodronate-liposome pretreatment abrogates myeloma tumor development *in vivo*. Clodronate-liposome administration resulted in depletion of CD169<sup>+</sup> bone marrow-resident macrophages. Flow cytometric analysis revealed that clodronate-liposome pretreatment impaired myeloma plasma cell homing and retention within the bone marrow 24 hours postmyeloma plasma cell inoculation. This was attributed in part to decreased levels of macrophage-derived insulin-like growth factor 1. Moreover, a single dose of clodronate-liposome led to a significant reduction in myeloma tumor burden in KaLwRij mice with established disease. Collectively, these findings support a role for CD169-expressing bone marrow-resident macrophages in myeloma disease establishment and progression and demonstrate the potential of targeting macrophages as a therapy for myeloma patients.

*Neoplasia* (2019) 21, 777–787

Address all correspondence to: Andrew Zannettino, Myeloma Research Laboratory, Adelaide Medical School, Faculty of Health and Medical Sciences, University of Adelaide, Cancer Theme, Level 5 South, SAHMRI, PO Box 11060, Adelaide, SA, Australia 5001.

E-mail: [andrew.zannettino@adelaide.edu.au](mailto:andrew.zannettino@adelaide.edu.au)

<sup>1</sup> co-senior author

Received 28 November 2018; Revised 27 May 2019; Accepted 28 May 2019  
© 2019 The Authors. Published by Elsevier Inc. on behalf of Neoplasia Press, Inc.  
This is an open access article under the CC BY-NC-ND license (<http://creativecommons.org/licenses/by-nc-nd/4.0/>).  
1476-5586  
<https://doi.org/10.1016/j.neo.2019.05.006>

## Introduction

Multiple myeloma (MM) is a plasma cell malignancy characterized by the clonal proliferation of aberrant plasma cells (PC) within the bone marrow (BM); accumulation of monoclonal immunoglobulin (paraprotein); and end-stage organ damage including osteolytic bone lesions, hypercalcemia, anemia, and renal insufficiency [1]. MM accounts for 1% of all cancers [2], with over 100,000 people diagnosed worldwide each year [3]. In almost all cases, MM is preceded by an indolent, asymptomatic disease known as monoclonal gammopathy of undetermined significance (MGUS), which is characterized by an increase in PC numbers within the BM (<10%) but manifests with few, if any, of the clinical features of symptomatic MM [4]. Despite advances in MM management and therapy, MM remains almost universally fatal.

In response to a chemokine gradient, MM PC home to the BM and colonize discrete endosteal niches within the medullary cavity, adjacent to bone surfaces [5]. Cells within the BM produce factors such as C-X-C motif chemokine ligand 12 (CXCL12; SDF-1) that increase the migration, adhesion, and retention of MM PC [6,7]. Recent data show that while many MM PC home to the BM, very few proliferate and contribute to the tumor burden [8,9]. This phenomenon is, at least in part, determined by the microenvironment in which these cells colonize. However, it is currently unclear what cell types within the BM contribute to the proliferative MM niche and which maintain MM cells in dormancy.<sup>2</sup>

Resident macrophages are heterogeneous immune cells of the mononuclear phagocytic lineage found in most adult tissues [10]. Within the BM, resident macrophages can be partitioned into distinct subpopulations based on their phenotype, anatomical location, and specialized function. Notably, macrophage numbers have previously been shown to increase in the BM of patients with active MM compared with asymptomatic MGUS [11] and have been associated with poor prognosis [12]. In addition, tumor-associated macrophages (TAMs) have been shown to promote angiogenesis, as well as MM PC growth and survival [13]. Interestingly, macrophages have been shown to directly contribute to the myeloma blood vessel network *via* “vasculogenic mimicry” [14] and are well documented to protect MM PC from drug-induced apoptosis [15–17]. Despite these findings, a direct role for BM resident macrophages in the establishment of MM remains unknown.

Interestingly, the depletion of mature macrophages using liposomal clodronate has shown promise as a therapy to inhibit tumor progression in a range of malignancies including lymphoma [18], melanoma [19], lung adenocarcinoma [20], and ovarian cancer [21]. The bisphosphonate clodronate, like other members of its class, is an antiresorptive agent that is rapidly and selectively adsorbed to bone following administration, limiting systemic exposure [22]. Encapsulation of clodronate in lipid vesicles specifically targets clodronate to phagocytic macrophages that engulf and degrade the liposome, leading to clodronate accumulation and subsequent cellular apoptosis [23]. Unlike free clodronate, clodronate-liposomes (clo-lip) globally deplete macrophages and other phagocytic cells [23,24].

In this study, the well-established C57BL/KaLwRijHsd (KaLwRij) murine model of myeloma was utilized in combination with clo-lip-mediated macrophage depletion to assess the role of mature macrophages in the initial establishment of MM PC within the BM. Furthermore, we assessed the efficacy of clo-lip as a potential therapy for MM. We found that clo-lip pretreatment led to a significant reduction in BM MM PC homing and retention, a concomitant increase in the numbers of circulating tumor cells, and decreased tumor burden. In addition, we characterized the effects of clo-lip on the BM microenvironment and investigated BM macrophages *in vitro* in order to elucidate the potential mechanisms by which clo-lip-mediated macrophage depletion impaired MM PC homing.

## Methodology

### Cell Culture

All cells were cultured under sterile conditions and maintained at 37°C with 5% CO<sub>2</sub>. Unless otherwise stated, all reagents were obtained from Sigma-Aldrich, St. Louis, MI. All media were supplemented with additives: 2 mM L-glutamine, 1 mM sodium pyruvate, 15 mM HEPES, 50 U/ml penicillin, and 50 µg/ml streptomycin. Mouse 5TGM1 MM PC, previously modified to express green fluorescent protein (GFP) and luciferase construct (luc) (5TGM1-eGFP-luc) [25,26], were maintained in complete Iscove's modified Dulbecco's medium (IMDM) supplemented with 20% fetal calf serum (FCS) (HyClone, QLD, Australia). A human BM endothelial cell (BMEC) line (TrhBMEC) was maintained in Medium 199 (M199) supplemented with 20% FCS, 0.01% sodium bicarbonate, 1× MEM nonessential amino acids (Life Technologies), 50 µg/ml endothelial cell growth supplement (BD Biosciences, Franklin Lakes, NJ), and 100 U/ml heparin.

### Animals

C57BL.KaLwRijHsd (KaLwRij) mice were bred and housed at the South Australian Health and Medical Research Institute (SAHMRI) Bioresearch facility. All studies were performed in accordance with SAHMRI Animal Ethics Committee approved procedures. Six- to 8-week-old age- and sex-matched KaLwRij mice were injected *i.v.* with a single dose of clo-lip or control phosphate-buffered saline (PBS)-liposome (PBS-lip) suspensions (200 µl/20 g mouse) (Liposoma BV, Amsterdam, the Netherlands) or *i.p.* with 100 µg/kg zoledronate (Novartis Pharma, Basel, Switzerland) and administered *i.v.* with 5×10<sup>5</sup> or, for the homing assay, 5×10<sup>6</sup> 5TGM1-eGFP-Luc cells in 100 µl of sterile PBS. Tumor development was monitored weekly by bioluminescence imaging (BLI) as previously described [27,28]. C57BL/6 mice were injected *i.v.* with a single dose of clo-lip or control PBS-lip suspensions (200 µl/20 g mouse) 24 hours prior to *i.v.* injection of 1×10<sup>6</sup> Vk\*MyC 4929 cells. At experimental endpoints, or weekly for the Vk\*MyC model, serum was isolated and serum paraprotein electrophoresis (SPEP) performed on a Sebia Hydragel b1/b2 kit (Sebia, Norcross, GA).

### Flow Cytometric Analysis

For BM detection of GFP<sup>+</sup> tumor cells, BM was flushed from the long bones using a 21G needle into PFE (PBS, 2% FCS, 2 mM ethylenediamine tetra-acetic acid [EDTA]), cut longitudinally with a scalpel blade, scraped along the inner surface, and finely chopped.

<sup>2</sup> BLI: bioluminescence imaging; BM: bone marrow; BMEC: BM endothelial cell; clo-lip: clodronate-liposome; HSC: hematopoietic stem cells; M-CSF: macrophage colony-stimulating factor; MGUS: monoclonal gammopathy of undetermined significance; MM: multiple myeloma; MSC: mesenchymal stem cells; PBS-lip: PBS-liposome; PC: plasma cells; SPEP: serum paraprotein electrophoresis; TAM: tumor-associated macrophage

Bone fragments were crushed and syringed several times before straining through a 70- $\mu$ m cell strainer, and the resulting cell suspension was pooled with the flushed BM. Cells were washed and resuspended in PFE for immediate analysis on an LRSFortessa X20 flow cytometer (BD Biosciences).

For circulating tumor cell analysis, mice were anesthetized by isoflurane inhalation and cardiac blood collected using a 26G needle containing 50  $\mu$ l 0.5 M EDTA to prevent clotting. Red blood cells were lysed by incubating three times with red blood cell lysis buffer (0.15 mM ammonium chloride, 10 mM potassium bicarbonate, and 1.26 mM disodium EDTA, pH 8.0) for 10 minutes. Cells were washed and resuspended in Hank's buffered saline solution with 5% FCS, filtered, and analyzed immediately on a BD FACS Canto II flow cytometer. In all instances, a BM or blood from a naive (noninjected) mouse was used as a negative control or was spiked with *in vitro*-cultured 5TGM1 cells for a GFP-positive control.

For cell lineage analysis, BM cells were extracted from long bones (femora and tibiae) using a mortar and pestle, stained with Fixable Viability Stain 700 (323 ng/ml; BD Biosciences), and blocked with mouse gamma globulin (117  $\mu$ g/ml; Abacus ALS, QLD, Australia). For detection of tumor cells in the Vk\*Mye model, BM was stained with CD138-PE (BioLegend, San Diego, CA) and B220-PE-Cy7 (eBioscience, San Diego, CA). For detection of BM macrophages, BM was stained with CD11b-APC Cy7, CD169-PE (BioLegend), and F4/80-Pacific Blue (Bio-Rad, Hercules, CA). For hematopoietic cells, mature Lin<sup>+</sup> cells were excluded by incubation with a lineage cocktail of biotin-conjugated antibodies (B220, CD3, CD4, CD5, CD8, Gr1, Ter119 [BioLegend] and Cd11b [eBioscience]) followed by streptavidin-APC (Life Technologies, Carlsbad, CA) secondary. Cells were concurrently stained with Sca-Brilliant Violet-(BV)786, cKit-PE-Cy7, CD135-PE-CF594, and CD34-BV421 (all from BD Biosciences). Mesenchymal cells were quantitated from compact bone as previously described [26]. Cells were either fixed in 1% neutral buffered formalin, 2% glucose, and 0.01% sodium azide in PBS or immediately analyzed on the LRSFortessa X20.

### Histological Analysis and TRAP staining

Femora were fixed in 10% paraformaldehyde, processed, and embedded in methacrylate as previously described [29]. Five-micron sections were cut and stained for the presence of tartrate-resistant acid phosphatase 5 (TRAP) to identify osteoclasts, as previously described [29]. Briefly, slides were deplasticized in acetone and incubated in AS-BI phosphate (0.4 mg/ml) in acetate-tartrate buffer (200 mM sodium acetate, 100 mM potassium sodium tartrate, pH 5.2) at 37°C for 30 minutes. The samples were then transferred to hexazotized pararosaniline solution (1 mg/ml) in prewarmed tartrate-acetate buffer and incubated for 30 minutes at 37°C. Sections were rinsed and counterstained with 0.05% methyl green solution. To enumerate osteoclasts, histomorphometric analysis was performed using the OsteoMeasure7 v4.1.0.2 analysis system (OsteoMetrics, Decatur, GA). Osteoclasts were defined based on TRAP-positive staining and the standard criterion of multinucleated cells ( $\geq 3$  nuclei) residing along the bone surface.

### In Vitro Cell Survival Assay

5TGM1-eGFP-Luc cells ( $1 \times 10^5$ ) were incubated in IMDM media supplemented with additives and 20% FCS with clo-lip or PBS-lip for 3 days. Cells were stained with Fixable Viability Stain 700 (323 ng/ml) and analyzed on LRSFortessa X20 flow cytometer.

### In Vitro Macrophage Maturation

Long bones (tibiae and femora) were excised from 7-week-old KaLwRij mice and BM flushed using a 21G needle. BM cells were seeded into flasks at  $2.6 \times 10^5$  cells/cm<sup>2</sup> in IMDM media supplemented with additives, 10% FCS, and 25 ng/ml recombinant mouse macrophage colony-stimulating factor (M-CSF; Lonza, Basel, Switzerland), and media were replaced every 2-3 days. Cells were harvested following 6 days of M-CSF treatment using Accutase (Sigma-Aldrich) as per manufacturer's instructions. Macrophages were stained with rat anti-mouse F4/80-FITC (Bio-Rad) and CD169-PE (BioLegend), or FITC rat IgG2b-isotype control and PE rat IgG2a-isotype control (BioLegend), respectively, and analyzed on LRSFortessa X20 flow cytometer (BD Biosciences).

### Matured Macrophage Conditioned Media

KaLwRij matured macrophages were seeded at  $1 \times 10^5$  cells/cm<sup>2</sup> in IMDM media supplemented with additives, 10% FCS, and 12.5 ng/ml M-CSF. After 24 hours, fresh media (without M-CSF) were added. Conditioned media were collected after a further 24 hours of culture, filtered through a 0.22- $\mu$ m filter, and stored at -80°C until required.

### Transendothelial Migration Assay

Migration assays were performed using 8- $\mu$ m polycarbonate membrane Transwells (Costar, Washington, DC) in a 24-well plate. BMECs were seeded into the upper chamber of Transwells at  $1 \times 10^4$  cells/well. After 48 hours, media were removed, BMECs were washed with serum free IMDM,  $1 \times 10^5$  5TGM1-eGFP-luc cells in IMDM media were supplemented with additives, and 10% FCS was added on top of the BMEC monolayer. Macrophage-derived conditioned media diluted to 10% and 50% in IMDM or IMDM medium alone were added to the lower chamber. The number of migrated 5TGM1-eGFP-luc cells was enumerated after 20 hours using an inverted microscope, digital camera (Olympus CKX41), and ImageJ software as described previously [30].

### Western Blot

5TGM1-eGFP-luc cells ( $2.5 \times 10^6$ ) were stimulated for 10 minutes with KaLwRij matured macrophage conditioned media or IGF-1 recombinant protein (ProSpec Bio, East Brunswick, NJ). Cell lysates were prepared, and equivalent amounts of protein (100  $\mu$ g) were separated on a 10% acrylamide gel and subjected to sodium dodecyl sulphate-polyacrylamide gel electrophoresis. Proteins were transferred to nitrocellulose membrane and subsequently blocked with 5% w/v skim milk. Immunoblotting was performed with antibodies directed against phospho-IGF-1R $\beta$  (Tyr1135/1136), IGF-1R $\beta$  (Cell signaling technologies, 1:1000), and  $\beta$ -Actin Clone AC-15 (Sigma-Aldrich, 1:2500). Following incubation with the appropriate IgG Dylight conjugated secondary antibodies (ThermoFisher, 1:20,000), proteins were visualized using the Odyssey Infrared Imaging System (LI-COR Bioscience, Lincoln, NE, USA).

### RNA Sequencing

Total RNA was extracted from 5TGM1-eGFP-luc cells using Trizol reagent (Life Technologies) according to the manufacturer's instructions. 5TGM1-eGFP-luc RNA was confirmed to be of adequate quality (RIN score >8) using a Bioanalyzer 2200 (Agilent), and samples were stored at -80°C. The cDNA libraries were prepared using NEXTflex mRNA-sequencing kit (BIOO Scientific) and

sequenced using a NextSeq500 sequencer (Illumina) at the David Gunn Genomics Facility (SAHMRI, Adelaide). Raw RNA-sequencing data (fastq files) of single-end reads ( $1 \times 75$  bp) were analyzed. Briefly, read quality was assessed using FastQC. Overrepresented adapter sequences were trimmed using Trimmomatic version 0.33, and quality assessment was repeated. Filtered reads were mapped to the reference genome hg19 using STAR version 2.5.0b. Aligned output data (BAM files) from individual lanes of the same sample were combined, and the number of mapped reads were counted using featureCounts (part of Rsubread version 1.12.6). Transcripts expressed at levels below five counts per million reads, in at least three libraries, were filtered out from downstream analysis. Relative expression was determined using quasi-likelihood *F* test from edgeR R package to account for variability due to relatively small sample size. Significantly regulated genes were identified using a cutoff of one-fold or greater changes in mean expression and FDR  $< 0.05$ .

### RNA Isolation and Quantitative Real-Time Polymerase Chain Reaction (PCR)

Total RNA was extracted from BM cells and KaLwRij matured macrophages using Trizol reagent (Life Technologies) according to the manufacturer's instructions. Following which, cDNA was synthesized using Superscript IV (Life Technologies) as per manufacturer's protocol. Gene-specific quantitative real-time PCR was conducted on a Bio-Rad CFX 9000 qPCR instrument using RT<sup>2</sup> SYBR Green reagent (QIAGEN, Hilden, Germany) and primer pairs as shown in Supplementary Table I. Resultant gene expression was analyzed using the  $\Delta\Delta C_t$  method ( $2^{-\Delta\Delta C_t}$ ) normalized to  $\beta$ -actin.

### Statistical Analysis

Statistical analyses were conducted using GraphPad Prism v 7.03. Groups were compared using one-way or two-way analysis of variance (ANOVA) with Tukey's or Holm-Sidak's multiple comparisons posttests or unpaired *t* tests as indicated.

## Results

### Clodronate-Liposome mediated Macrophage depletion

Clo-lip has previously been shown to globally deplete mature, functional macrophages [23,31,32]. Initially, we confirmed the effect of clo-lip on BM macrophages in tumor-naïve KaLwRij mice. Mice were treated with a single i.v. injection of clo-lip or a PBS-lip control, and the extent of macrophage depletion was investigated. As clo-lip administration is known to induce apoptosis of all phagocytic cells, including osteoclasts [24], zoledronate was administered to a third group of mice as an osteoclast-depletion control [33]. Flow cytometric analysis revealed a 70% reduction in the total CD11b<sup>+</sup>F4/80<sup>+</sup> monocyte/macrophage population within the BM of clo-lip-treated animals compared with controls (Figure 1A). Notably, this decrease was due solely to the ablation of the CD11b<sup>+</sup>F4/80<sup>+</sup>CD169<sup>+</sup> mature BM macrophage population, which was reduced by 90% in the clo-lip-treated mice compared with PBS-lip and zoledronate controls, while the CD11b<sup>+</sup>F4/80<sup>+</sup>CD169<sup>-</sup> monocyte/macrophage population was unaffected by clo-lip treatment (Figure 1, A and B). Importantly, the depletion of BM macrophages was maintained for more than 14 days, with the CD169<sup>+</sup> macrophage population only returning to 50% of that of control animals 28 days after a single i.v. injection of clo-lip (Figure 1C).

### Inhibition of MM Tumour Development by Clodronate-Liposome Pretreatment

To investigate the effect of clo-lip-mediated macrophage ablation on MM tumor development, KaLwRij mice were inoculated with 5TGM1 MM PC *via* the tail vein 24 hours after the mice had been treated with clo-lip, PBS-lip, or zoledronate. Zoledronate-treated mice developed tumor at a similar rate to PBS-lip-treated mice, indicating that inhibition of osteoclasts does not affect tumor establishment and growth in this model. In contrast, clo-lip pretreatment resulted in a significantly reduced tumor burden compared with PBS-lip controls (Figure 2). Mice treated with clo-lip displayed  $>95\%$  lower tumor burden as determined by both BLI (Figure 2, A and B) and SPEP analysis (Figure 2C) after 4 weeks. In addition, flow cytometric analysis at 4 weeks post tumor cell inoculation revealed a significant decrease in the number of GFP<sup>+</sup> tumor cells in the circulation (Figure 2D) of clo-lip-treated mice compared with controls. Notably, comparable results were observed in the progressive Vk\*Myb MM murine model following upfront clo-lip treatment (Figure S1).

Interestingly, although there was a significant decrease in the total number of GFP<sup>+</sup> tumor cells in the BM of clo-lip-treated KaLwRij mice at day 28, there was no difference in the tumor growth rate between the two treatment groups from day 14 to day 28 [population doublings: PBS-lip,  $8.9 \pm 0.2$ ; clo-lip,  $8.4 \pm 0.4$  (mean  $\pm$  SD;  $P = .24$ )] (Figure S2). Moreover, 5TGM1 cell viability was not affected by 72 hours of clo-lip treatment *in vitro* (Figure S3). Together, these data suggest that the inhibition of tumor development in clo-lip-treated animals was not due to direct effects on 5TGM1 cell growth or survival.

### Effect of Clodronate-Liposomes on MM PC Homing and Retention in the BM

The homing of MM PC to specific niches within the BM that support their colonization and growth is a critical event in the establishment of MM tumors [5,9]. As there was no effect on MM PC proliferation or survival following clo-lip treatment, we next investigated the effect of clo-lip-mediated macrophage depletion on 5TGM1 MM PC homing and retention. 5TGM1 MM PC were injected i.v. into clo-lip- or PBS-lip-treated mice, and the number of GFP<sup>+</sup> tumor cells present within the BM and peripheral blood was assessed after 24 hours by flow cytometry. A 2.7-fold reduction in the total number of tumor cells present within the BM of clo-lip-treated mice was observed (Figure 3A), with a concomitant 5.4-fold increase in the number of tumor cells remaining in circulation (Figure 3B), compared with PBS-lip-treated controls. Collectively, these data suggest that clo-lip treatment impairs MM development *in vivo*, at least in part, by inhibiting MM PC homing to and/or retention within the BM.

### Role of Macrophages in MM PC Migration

As clo-lip treatment inhibited the homing of MM PC to the BM, we next investigated whether macrophages play a specific role in MM PC migration. Macrophages were matured *in vitro* from KaLwRij BM by treatment with macrophage-colony stimulating factor (M-CSF) for 6 days. As confirmed by flow cytometric assessment at day 6, more than 90% of the matured cells were F4/80<sup>+</sup>, and on average, 42% were CD169<sup>+</sup> (Figure S4). Conditioned media from these KaLwRij matured macrophages stimulated 5TGM1 MM PC

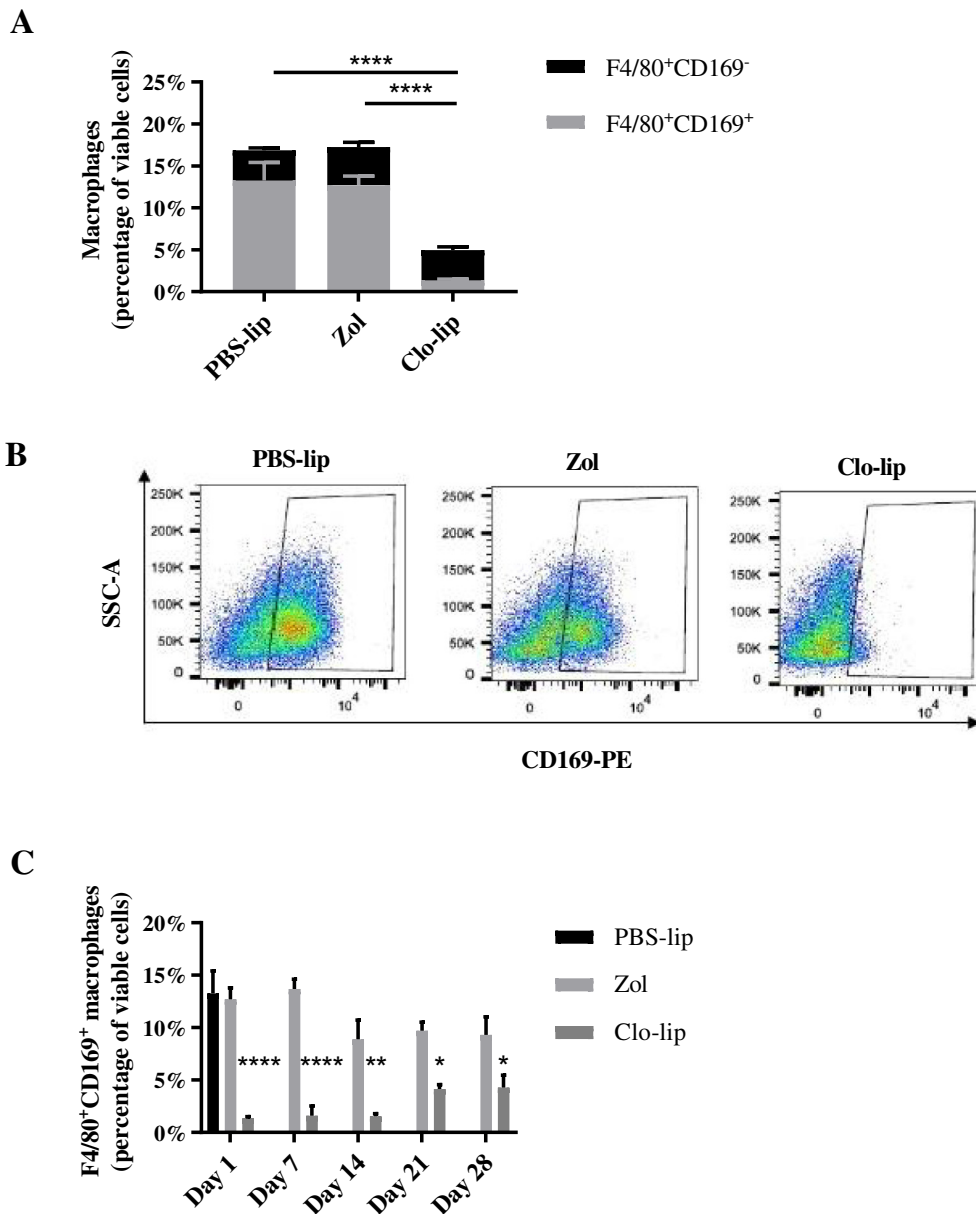


**Fig. 1.** Clodronate-liposomes deplete CD169-expressing macrophages within the BM. KaLwRij mice were treated once with PBS-lip, zol, or clo-lip. Total BM was isolated from long bones after 24 hours (A, B) or as indicated (C); stained with Cd11b, F4/80, and CD169 fluorescently conjugated antibodies; and analyzed by flow cytometry. (A) Cd11b<sup>+</sup>F4/80<sup>+</sup>CD169<sup>-</sup> monocyte/macrophage population (black; n.s.,  $P = .694$ ) and Cd11b<sup>+</sup>F4/80<sup>+</sup>CD169<sup>+</sup> mature macrophages (gray; \*\*\*\* $P < .0001$ ) expressed as a percentage of total viable cells. (B) Representative FACS plots of Cd11b<sup>+</sup>F4/80<sup>+</sup>CD169<sup>+</sup> mature macrophages. (C) Recovery of Cd11b<sup>+</sup>F4/80<sup>+</sup>CD169<sup>+</sup> mature macrophages following a single injection of clo-lip over a 28-day period.  $n = 3/\text{group}$ . Graphs show mean  $\pm$  SEM, \* $P < .05$ , \*\* $P < .01$ , \*\*\*\* $P < .0001$ , 2-way ANOVA with Tukey's multiple comparisons test.

migration in a dose-dependent manner (Figure 4A), suggesting that macrophages play a direct role in MM PC homing and migration.

To further investigate the potential mechanism by which macrophages increase MM PC migration *in vitro*, the expression of chemokine/cytokine receptors for key secreted factors that play a role in MM pathogenesis was assessed in 5TGM1 cells by RNAseq. Notably, 5TGM1 cells expressed high levels of the insulin-like growth factor 1 (IGF-1) receptor (*Igf1r*), the receptors for BAFF (TNFSF13B) and APRIL (TNFSF13) (*Tnfrsf13b* and *Tnfrsf13c*), the receptor for CXCL12 (*Cxcr4*), the receptor for tumor necrosis factor alpha (TNF- $\alpha$ ) (*Tnfrsf1a*), and the genes encoding the interleukin 6

(IL-6) receptor complex (*Il6st* and *Il6ra*) (Figure 4B and Supplementary Table II).

Next, the mRNA expression levels of the corresponding ligands were analyzed in KaLwRij matured BM macrophages. Notably, high levels of *Igf1* mRNA (Figure 4C), a potent promigratory and proliferative factor for MM PC [34,35], were observed. In contrast, KaLwRij matured BM macrophages expressed low levels of *Tnfa* and *Tnfsf13* and undetectable *Il6*, *Tnfsf13b*, and *Cxcl12* (Figure 4C). Next, we confirmed the expression and activation of IGF-1R in 5TGM1 cells by Western blot. As shown in Figure 4D, recombinant IGF-1 protein stimulated a dose-dependent phosphorylation of IGF-

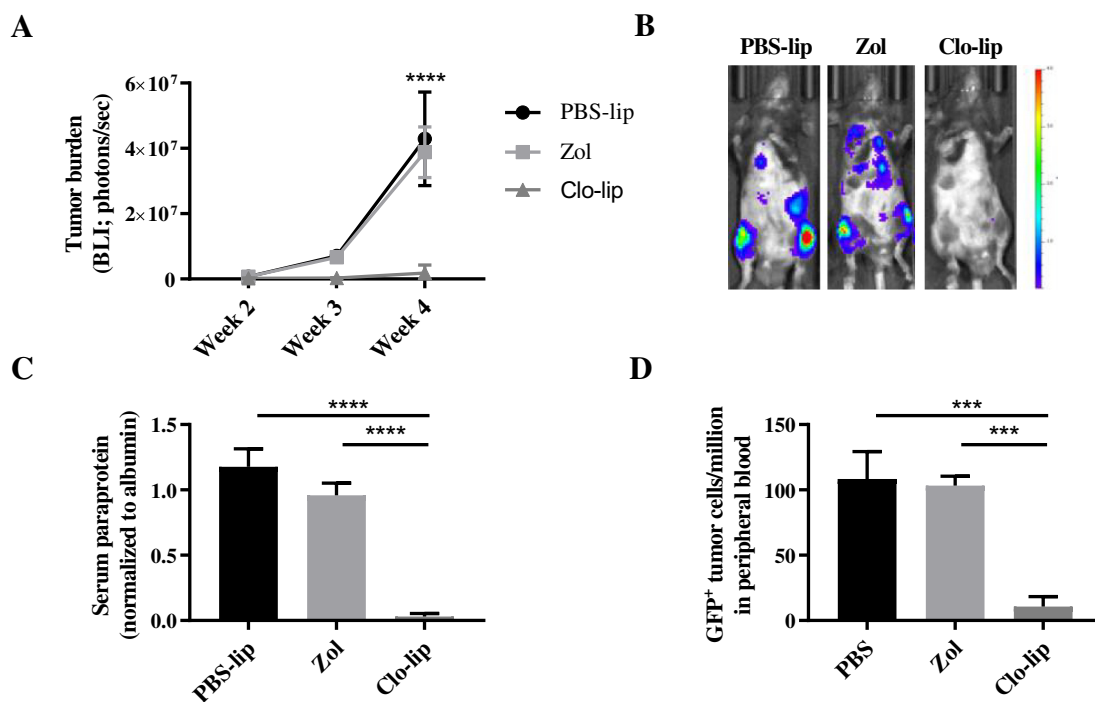


**Fig. 2.** Clodronate-liposome pretreatment inhibits MM tumor development *in vivo*. KalwRij mice were treated once with PBS-lip, zol, or clo-lip 24 hours prior to i.v. injection of 5TGM1 MM PC. (A) Tumor burden was measured by BLI at 2, 3, and 4 weeks post tumor cell inoculation. Graph shows mean  $\pm$  SEM, \*\*\*\* $P$  < .0001, two-way ANOVA with Tukey's multiple comparisons test. (B) Representative BLI images for each treatment group at 4 weeks. (C) Serum paraprotein quantitation at 4 weeks. (D) Flow cytometric analysis of GFP+ 5TGM1 within the peripheral circulation at 4 weeks.  $n = 3$ –8/group. Graphs show mean  $\pm$  SEM, \*\*\* $P$  < .001, \*\*\*\* $P$  < .0001, 1-way ANOVA with Tukey's multiple comparisons test.

1R in 5TGM1 cells. Moreover, stimulation with matured macrophage conditioned medium also resulted in IGF-1R phosphorylation (Figure 4E), confirming that macrophage conditioned medium contains IGF-1. Taken together, these data suggest that macrophage-derived IGF-1 may play an important role in 5TGM1 MM PC migration.

#### Clodronate-Liposome Treatment Decreases BM-Expressed *Igf1* and *Cxcl12* *In Vivo*

In order to investigate whether clo-lip treatment alters the mRNA expression profile within the BM, the expression of MM-associated

chemokines and cytokines, identified above, was assessed by qPCR on total BM 24 hours after clo-lip or PBS-lip treatment. Interestingly, there was a significant decrease in *Igf1* mRNA levels in clo-lip-treated animals compared with PBS-lip controls (Figure 5A). In addition, BM expression of *Cxcl12*, which plays an important role in MM PC homing, retention, and growth [36], was significantly decreased following clo-lip treatment (Figure 5B). In contrast, no change in the mRNA levels of *Tnfsf13b*, *Tnfsf13*, *Tnfa*, or *Il6* was observed (Figure 5, C-F). These findings suggest that MM PC migration may be impaired, at least in part, *via* clo-lip-mediated reduction in BM levels of IGF-1 and CXCL12.

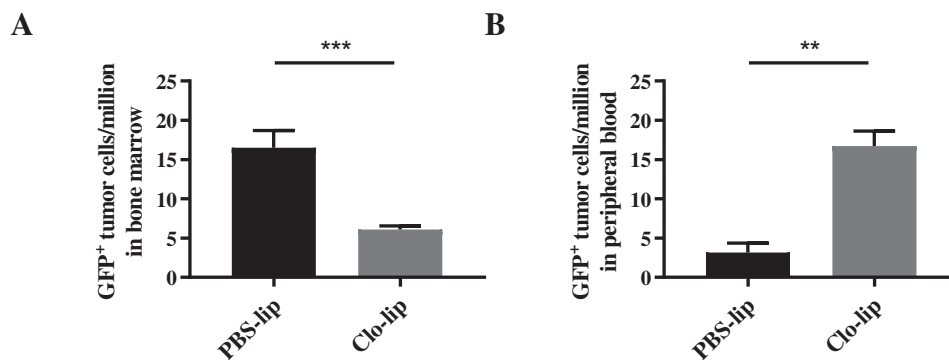


**Fig. 3.** Clodronate-liposome pretreatment impairs MM PC homing/retention *in vivo*. GFP+ 5TGM1 MM PC within the (A) BM or (B) in the circulation 24 hours after tumor cell inoculation were analyzed by flow cytometry in PBS-lip- or clo-lip-treated mice.  $n = 3$ –5/group. Graph shows mean  $\pm$  SEM, \*\* $P$  < .01, \*\*\* $P$  < .001, unpaired  $t$  test.

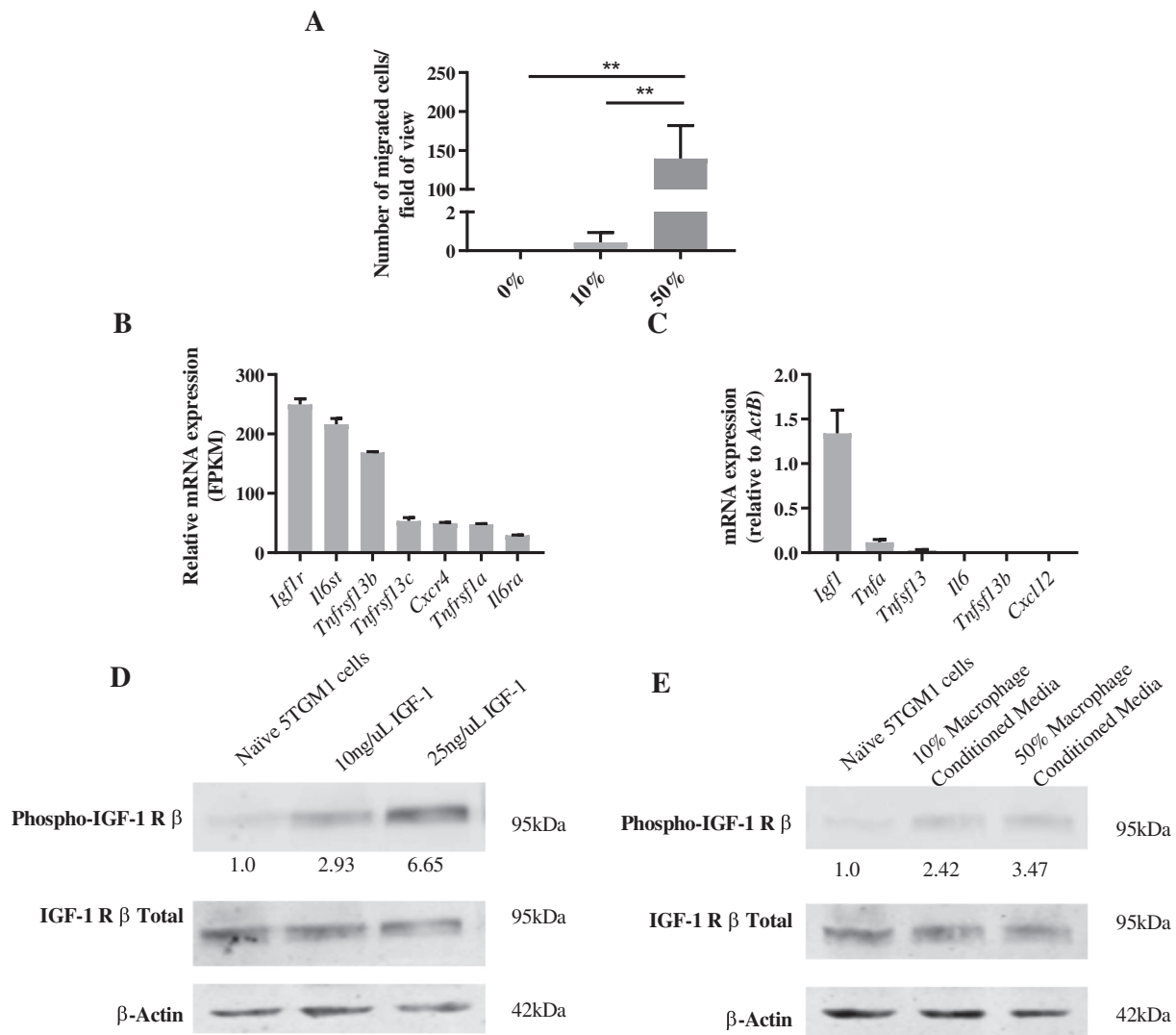


**Fig. 4.** IGF-1-expressing KaLwRij matured macrophages enhance MM PC migration *in vitro*. (A) Transendothelial migration of 5TGM1 MM PC toward increasing concentrations of KaLwRij matured BM macrophage conditioned media. Graph shows mean  $\pm$  SD,  $n = 3$ ;  $^{**}P < .01$ , 1-way ANOVA with Tukey's multiple comparisons test. (B) Relative mRNA gene expression of cell surface receptors on 5TGM1 MM PCs by RNAseq analysis. (C) Relative mRNA gene expression of KaLwRij matured BM macrophages analyzed by qPCR. Graphs show mean  $\pm$  SD,  $n = 3$ . (D) Western blot analysis of 5TGM1 MM PC stimulated for 10 minutes with increasing concentrations of IGF-1 recombinant protein or (E) KaLwRij matured BM macrophage conditioned media. Numbers indicate fold change in phospho-IGF-1R relative to total IGF-1R, normalized to naive. Images are representative of three independent experiments.

#### Clodronate-Liposomes Decrease Osteoblast Numbers *In Vivo*

As both macrophages and osteoclasts are an abundant source of IGF-1 [37,38], we assessed osteoclast numbers 24 hours post clo-lip and PBS-lip administration. There was no significant difference in the number of osteoclasts (No.Oc/B.Pm) in clo-lip-treated mice compared to PBS-lip controls ( $P = .71$ ,  $t$  test, Figure S5A). Notably, CXCL12 is not expressed by matured BM macrophages (Figure 4C) but is produced in the BM by cells of the mesenchymal lineage, including MSCs and osteoblasts [36]. Changes in MSC, osteoprogenitor, and osteoblast numbers within the compact bone following 24 hours of clo-lip exposure were investigated by flow cytometry. Following exclusion of hematopoietic (CD45/Lin) and endothelial (CD31) cells, mesenchymal cell populations were resolved based on their expression of CD51 and Sca1 [26,39]. While clo-lip treatment had no effect on MSC [CD45<sup>-</sup>Lin<sup>-</sup>CD31<sup>-</sup>CD51<sup>-</sup>Sca1<sup>+</sup>] numbers, a 6.5-fold decrease in osteoprogenitors [CD45<sup>-</sup>Lin<sup>-</sup>CD31<sup>-</sup>CD51-

<sup>+</sup>Sca1<sup>-</sup>] and 7.5-fold decrease in osteoblasts [CD45<sup>-</sup>Lin<sup>-</sup>CD31<sup>-</sup>CD51<sup>+</sup>Sca1<sup>+</sup>] were observed in clo-lip-treated mice compared with PBS-lip-treated controls (Figure S5B). These data suggest that decreased osteoblast numbers may account for the reduction in *Cxcl12* mRNA observed in the BM of clo-lip-treated mice.

#### Hematopoietic Lineage Cells Increase *In Vivo* Following Clodronate-Liposome Treatment

As shown above, clo-lip administration dramatically decreased osteoblast and osteoprogenitor cell numbers, which in addition to playing a role in myeloma pathogenesis are also a key component of the hematopoietic stem cell (HSC) niche [40]. Therefore, we also investigated clo-lip-mediated changes to hematopoietic progenitor cell numbers within the BM. Hematopoietic cell populations were resolved based on their expression of CD135 and CD34. Clo-lip treatment resulted in a significant 5-fold increase in hematopoietic

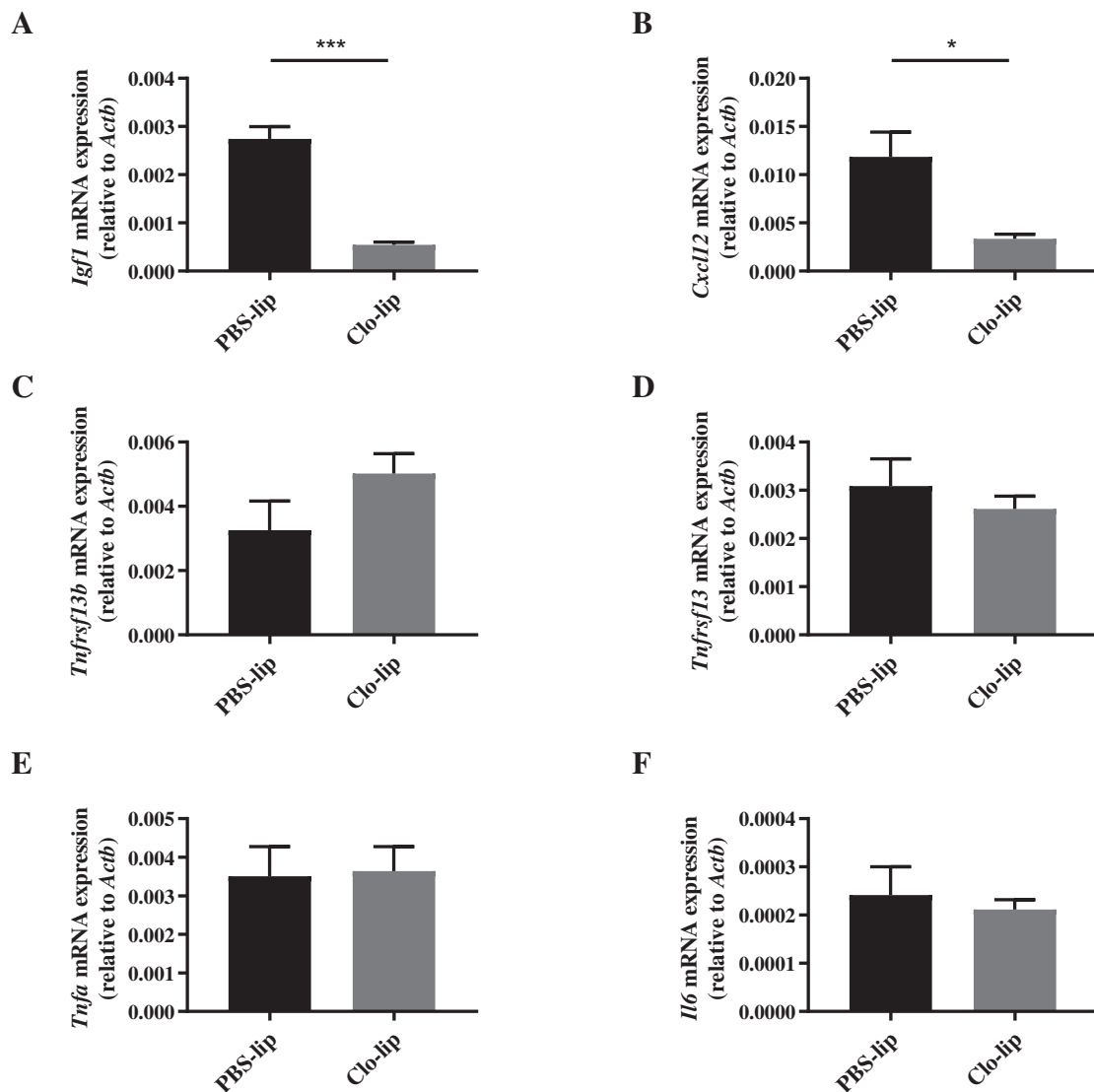


**Fig. 5.** Clodronate-liposome pretreatment affects the mRNA expression profile of the BM. KaLwRij mice were injected i.v. with PBS-lip or clo-lip, and 24 hours later, BM was harvested from tibiae and femora for assessment of (A) *Igf1*, (B) *Cxcl12*, (C) *Tnfrsf13b*, (D) *Tnfrsf13*, (E) *Tnfa*, and (F) *Il6* gene expression by qPCR. Graphs show mean  $\pm$  SEM,  $n = 3-4$ /group; \* $P < .05$ , \*\*\* $P < .001$ , unpaired  $t$  test.

stem/progenitor cells (HSPC) [ $\text{Lin}^- \text{Sca-1}^+ \text{cKit}^+$ ], a 2-fold increase in long-term HSC (LT-HSC) [ $\text{Lin}^- \text{Sca-1}^+ \text{cKit}^+ \text{CD135}^- \text{CD34}^-$ ], and a 12-fold increase in short-term HSC (ST-HSC) [ $\text{Lin}^- \text{Sca-1}^+ \text{cKit}^+ \text{CD135}^- \text{CD34}^+$ ] numbers when compared with PBS-lip-treated controls (Figure S5C). These data suggest that, in addition to MM tumor inhibition, clo-lip-mediated macrophage ablation may have downstream effects on the cellular composition of the BM microenvironment.

#### Reduction of MM Tumor Development Following Clodronate-Liposome Treatment In Vivo

To assess whether clo-lip-mediated ablation of macrophages may display therapeutic efficacy in the established disease setting, KaLwRij mice were inoculated with 5TGM1 MM PC and, 2 weeks later, injected with clo-lip or PBS-lip. Notably, clo-lip-treated mice demonstrated a 2.7-fold reduction in tumor burden at 4 weeks, compared with PBS-lip controls, as assessed by BLI (Figure 6, A-B) and SPEP (Figure 6C). Additionally, flow cytometric analysis

demonstrated a corresponding 4.5-fold decrease in the number of GFP<sup>+</sup> 5TGM1 tumor cells within the peripheral circulation at 4 weeks post tumor cell inoculation in clo-lip-treated mice compared with controls (Figure 6D). Interestingly, even in the presence of tumor, macrophage ablation was maintained, with the CD11b<sup>+</sup>F480<sup>+</sup>CD169<sup>+</sup> BM-resident macrophage population depleted by 90% 2 weeks post clo-lip treatment (Figure S6).

#### Discussion

The migration of MM PC to the BM and their subsequent proliferation and survival are well established to be dependent on supportive elements within the BM microenvironment. MM PC leave the peripheral lymphoid organ, enter the circulation, transendothelially migrate, and home to the BM in response to a chemokine gradient wherein they colonize discrete endosteal niches. Here, the MM PC interact with cells of the BM microenvironment, which secrete pro-proliferative and antiapoptotic cytokines that favor MM PC growth and survival within the BM [5,36]. While macrophages



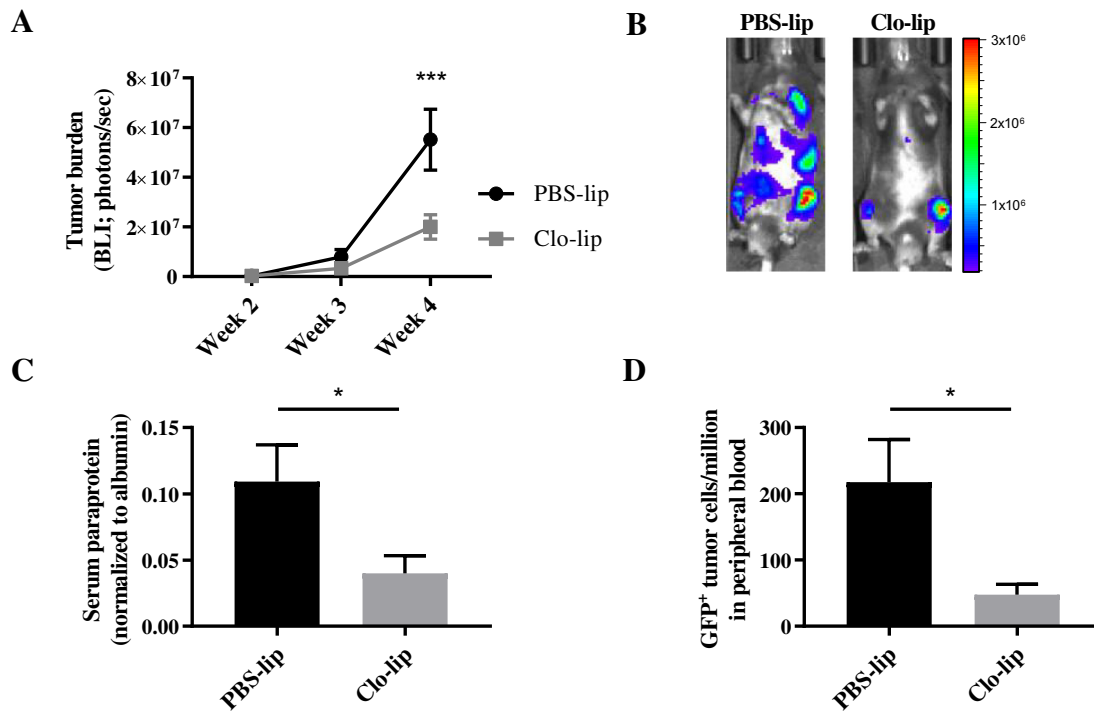


**Fig. 6.** MM tumor development is significantly reduced *in vivo* in clodronate-liposome-treated mice. KaLwRij mice were inoculated i.v. with 5TGM1 MM tumor cells, and tumor was allowed to establish for 2 weeks, followed by a single treatment with PBS-lip or clo-lip ( $n = 7$ /group). (A) Tumor burden was measured by BLI at 2, 3, and 4 weeks post tumor cell inoculation. Graph shows mean  $\pm$  SEM,  $***P < .001$ , two-way ANOVA with Sidak's multiple comparisons test. (B) Representative BLI images for each treatment group at week 4. (C) Serum paraprotein quantitation 4 weeks post tumor cell inoculation. (D) Flow cytometric analysis of GFP<sup>+</sup> 5TGM1 within the peripheral circulation at 4 weeks post tumor cell inoculation. Graphs show mean  $\pm$  SEM;  $*P < .05$ , unpaired  $t$  test.

have been suggested to play a role in this process, infiltrating the established MM tumor [13], the role of BM-resident macrophages in MM PC colonization and disease establishment has not been fully elucidated. Liposome-encapsulated clodronate, which depletes macrophages and other phagocytic cells, has previously been shown to inhibit tumor progression in a range of cancers [18–21]. In this study, we demonstrate, for the first time, that clo-lip-mediated ablation of the mature CD11b<sup>+</sup>F4/80<sup>+</sup>CD169<sup>+</sup> BM macrophage population in the 5TGM1/KaLwRij murine model of MM significantly impairs MM tumor establishment, suggesting that CD169<sup>+</sup> BM-resident macrophages may play a pivotal role in MM pathogenesis.

In support of these findings, a recent study has shown that depletion of monocyte/macrophage lineage cells in MM tumor-bearing mice, by targeting CSF1R genetically or with a function-blocking anti-CSF1R antibody, significantly decreased MM tumor burden [16]. While our study confirmed that macrophages play a role in disease progression, we have also demonstrated a novel role for mature macrophages resident within the BM microenvironment in the initial stages of MM establishment. Moreover, we demonstrated that these mature BM-resident macrophages specifically express CD169 and play a critical role in MM PC homing and colonization within the BM.

In addition to a drastic reduction in tumor burden following upfront treatment with clo-lip, we also observed a significant decrease in tumor burden following the administration of clo-lip in the established disease setting. The dissemination of MM PC to sites throughout the BM is an essential process in MM disease progression and relapse, and parallels various features of solid tumor metastasis to

bone [41]. We propose that the decreased tumor burden in the established setting may be attributed to a reduction in the dissemination of MM PC to secondary sites. Several studies have shown that liposomal clodronate results in decreased metastasis of solid tumors [42,43]. Moreover, clo-lip treatment in an intratibial model of prostate cancer perturbed tumor growth within the bone [44]. Together, these studies suggest that macrophages resident within the BM may play an important role in the development of solid tumor metastases within the bone.

To our knowledge, we present for the first time that BM macrophage conditioned medium was a potent inducer of 5TGM1 MM PC migration *in vitro*, suggesting that macrophage secreted factors may play a direct role in increasing the homing of 5TGM1 MM PC to the BM *in vivo*. While 5TGM1 MM PC express a number of receptors for cytokines and growth factors that may increase migration and proliferation, the predominant factor expressed at the mRNA level in KaLwRij BM-derived macrophages was *Igf1*, which is consistent with previous studies [38]. Notably, *Igf1* mRNA levels were also significantly reduced in the total BM of clo-lip-treated mice compared with PBS-lip controls, suggesting that clo-lip negatively affects MM PC homing and establishment, in part, by downregulation of BM IGF-1 levels, likely through direct depletion of IGF-1-expressing macrophages. IGF-1 is an important mitogenic and survival factor for MM PC [34] and has been suggested to be an important promigratory and adhesion factor in MM [35,45].

Consistent with previous studies, we have shown that global phagocytic cell depletion has secondary effects on other BM cells, inducing a rapid decrease in osteoblast and osteoprogenitor numbers

and a dramatic increase in HSCs [31,32,46,47]. IGF-1 has previously been shown to induce osteoblast differentiation [48], and as such, a decrease in *Igf1* may also account for the reduction in osteoblast and osteoprogenitor numbers observed in this study. Although interesting, this decrease in osteoblast number following clo-lip treatment is unlikely to account for the reduction in tumor burden, as studies show that osteoblasts may inhibit MM cell proliferation and survival [49]. Moreover, dormant MM PC reside near osteoblasts *in vivo*, suggesting that osteoblasts play a role in inducing MM PC quiescence rather than proliferation [9].

However, the decrease in osteoblasts observed here may result in changes in BM cytokine levels that decrease MM PC homing *in vivo*. Consistent with previous studies [31], clo-lip treatment was associated with a decrease in BM expression of *Cxcl12* mRNA. Although not expressed by macrophages, CXCL12 is expressed by MSCs and osteoblasts [36], suggesting that the decrease in BM CXCL12 levels may be secondary to the decrease in osteoblast numbers observed in this study. Additionally, BM macrophages have been shown to produce secreted factors that increase CXCL12 production by BM stromal cells *in vitro* [31], suggesting that ablation of BM macrophages may also decrease BM stromal cell CXCL12 production. CXCL12 secretion from stromal cells is known to play a key role in the BM recruitment and retention of MM PC from the peripheral blood [6,7] and CXCL12 induces 5TGM1 cell migration *in vitro* [27]. Interestingly, IGF-1 and CXCL12 have striking synergistic effects on the migration of human MM cell lines *in vitro* [50], suggesting that the decrease in the BM levels of both IGF-1 and CXCL12 may account for the dramatic effect on the BM homing of MM PC seen here in clo-lip-treated mice.

In addition to affecting the production of macrophage- and mesenchymal cell-derived chemokines, macrophage depletion may affect MM PC establishment in the BM by increasing the abundance of other cells in the BM that may crowd out MM PC. Flow cytometric analysis revealed a dramatic increase in the number of long term, short term, and progenitor HSCs within the BM of clo-lip-treated mice compared with PBS-lip controls. This finding supports previous studies that demonstrated a role for BM macrophages in maintaining the HSC niche [31,32,46,47]. Moreover, CXCL12 has been shown to be important in maintaining the quiescent HSC pool [51], and therefore, decreased *Cxcl12* levels within the BM following clo-lip treatment may result in HSC proliferation. While the MM PC proliferative niche is incompletely characterized, it is thought that there are overlaps between the niches occupied by HSCs and proliferating MM PC in the BM [36,52]. We speculate that the dramatic increase in the number of hematopoietic lineage cells within the BM following clo-lip treatment may disrupt the ability of MM PC to colonize supportive niches in the BM; however, further studies are required to confirm this.

This is the first study to demonstrate that CD169-expressing BM-resident macrophages play an instrumental role in the initial homing and establishment of MM disease. Moreover, we confirmed a requirement for macrophages in MM disease progression. Our findings also demonstrate that macrophages produce factors, including IGF-1, that increase the migratory capacity of MM PC. Further, we show that clo-lip-mediated macrophage depletion leads to demonstrable changes to the mesenchyme, leading to a reduction in *Cxcl12* expression, a factor important in MM PC homing and retention. Taken together, these studies highlight the potential of targeting BM-resident macrophages as a novel therapy for MM in the established and relapsed disease setting.

Supplementary data to this article can be found online at <https://doi.org/10.1016/j.neo.2019.05.006>.

## Acknowledgements

The authors would like to acknowledge Randall Grose of the ACRF Flow Facility, SAHMRI, and Alison Pettit and Susan Millard of the Bones and Immunology group, Mater Research Institute-University of Queensland, for their contributions to this work.

## Funding

This research was supported by a National Health & Medical Research Council Project Grant [A.C.W.Z., P.C., P.J.P., J.E.N.; APP1140996]. K. V. was supported by an Early Career Cancer Research Fellowship from the Cancer Council SA Beat Cancer Project on behalf of its donors and the State Government of South Australia through the Department of Health. P. J. P. was supported by a National Heart Foundation of Australia Future Leader Fellowship [FLF100412]. J. E. N. was supported by a Veronika Sacco Clinical Cancer Research Fellowship from the Florey Medical Research Foundation, University of Adelaide.

## Contributions

K. S. O. and J. E. N. performed majority of the research. K. C. C., E. A. C., D. R. H., and K. M. M. assisted with data generation. K. S. O., K. V., and J. E. N. performed data analysis. A. C. W. Z., J. E. N., K. V., and K. S. O. designed experiments and contributed substantially to the research project. A. E., N. S., and P. I. C. assisted with experimental design. K. S. O. wrote the manuscript. K. V., D. R. H., K. M. M., P. J. P., J. E. N. and A. C. W. Z. reviewed the manuscript, and J. E. N., P. J. P., and A. C. W. Z. supervised the study.

## Declarations

The authors declare that they have no competing interests.

## References

- [1] Kumar SK, Rajkumar V, Kyle RA, van Duin M, Sonneveld P, Mateos MV, Gay F, and Anderson KC (2017). Multiple myeloma. *Nat Rev Dis Primers* 3:17046.
- [2] Moreau P, Attal M, and Facon T (2015). Frontline therapy of multiple myeloma. *Blood* 125, 3076–3084.
- [3] Ferlay J, Soerjomataram I, Dikshit R, Eser S, Mathers C, Rebelo M, Parkin DM, Forman D, and Bray F (2015). Cancer incidence and mortality worldwide: sources, methods and major patterns in GLOBOCAN 2012. *Int J Cancer* 136, E359–386.
- [4] Landgren O, Kyle RA, Pfeiffer RM, Katzmann JA, Caporaso NE, Hayes RB, Dispenzieri A, Kumar S, Clark RJ, and Baris D, et al (2009). Monoclonal gammopathy of undetermined significance (MGUS) consistently precedes multiple myeloma: a prospective study. *Blood* 113, 5412–5417.
- [5] Manier S, Sacco A, Leleu X, Ghobrial JM, and Roccaro AM (2012). Bone marrow microenvironment in multiple myeloma progression. *J Biomed Biotechnol* 2012, 1–5.
- [6] Alsayed Y, Ngo H, Runnels J, Leleu X, Singha UK, Pitsillides CM, Spencer JA, Kimlinger T, Ghobrial JM, and Jia X, et al (2007). Mechanisms of regulation of CXCR4/SDF-1 (CXCL12)-dependent migration and homing in multiple myeloma. *Blood* 109, 2708–2717.
- [7] Vandyke, K., Zeissig, M.N., Hewett, D.R., Martin, S.K., Mrozik, K.M., Cheong, C.M., Diamond, P., To, L.B., Gronthos, S., Peet, D.J., Croucher, P.I. & Zannettino, A.C.W. (2017) HIF-2alpha promotes dissemination of plasma cells in multiple myeloma by regulating CXCL12/CXCR4 and CCR1. *Cancer Res* 77, 5452–5463.
- [8] Hewett DR, Vandyke K, Lawrence DM, Friend N, Noll JE, Geoghegan JM, Croucher PI, and Zannettino ACW (2017). DNA barcoding reveals habitual clonal dominance of myeloma plasma cells in the bone marrow microenvironment. *Neoplasia* 19, 972–981.
- [9] Lawson MA, McDonald MM, Kovacic N, Hua Khoo W, Terry RL, Down J, Kaplan W, Paton-Hough J, Fellows C, and Pettitt JA, et al (2015). Osteoclasts control reactivation of dormant myeloma cells by remodelling the endosteal niche. *Nat Commun* 6, 8983.
- [10] Davies LC and Taylor PR (2015). Tissue-resident macrophages: then and now. *Immunology* 144, 541–548.
- [11] Sponaas AM, Moen SH, Liabakk NB, Feyzi E, Holien T, Kvam S, Groseth LA, Stordal B, Buene G, and Espevik T, et al (2015). The proportion of CD16(+) CD14(dim) monocytes increases with tumor cell load in bone marrow of patients with multiple myeloma. *Immun Inflamm Dis* 3, 94–102.

- [12] Suyani E, Suck GT, Akyurek N, Sahin S, Baysal NA, Yagci M, and Haznedar R (2013). Tumor-associated macrophages as a prognostic parameter in multiple myeloma. *Ann Hematol* **92**, 669–677.
- [13] Ribatti D, Moschetta M, and Vacca A (2014). Macrophages in multiple myeloma. *Immunol Lett* **161**, 241–244.
- [14] Scavelli C, Nico B, Cirulli T, Ria R, Di Pietro G, Mangieri D, Bacigalupo A, Mangialardi G, Coluccia AM, and Caravita T, et al (2008). Vasculogenic mimicry by bone marrow macrophages in patients with multiple myeloma. *Oncogene* **27**, 663–674.
- [15] De Beule N, De Veirman K, Maes K, De Bruyne E, Menu E, Breckpot K, De Raeve H, Van Rampelbergh R, Van Ginderachter JA, and Schots R, et al (2017). Tumour-associated macrophage-mediated survival of myeloma cells through STAT3 activation. *J Pathol* **241**, 534–546.
- [16] Wang Q, Lu Y, Li R, Jiang Y, Zheng Y, Qian J, Bi E, Zheng C, Hou J, and Wang S, et al (2018). Therapeutic effects of CSF1R-blocking antibodies in multiple myeloma. *Leukemia* **32**, 176–183.
- [17] Zheng Y, Cai Z, Wang S, Zhang X, Qian J, Hong S, Li H, Wang M, Yang J, and Yi Q (2009). Macrophages are an abundant component of myeloma microenvironment and protect myeloma cells from chemotherapy drug-induced apoptosis. *Blood* **114**, 3625–3628.
- [18] Shen L, Li H, Shi Y, Wang D, Gong J, Xun J, Zhou S, Xiang R, and Tan X (2016). M2 tumour-associated macrophages contribute to tumour progression via legumain remodelling the extracellular matrix in diffuse large B cell lymphoma. *Sci Rep* **6**, 30347.
- [19] Piaggio F, Kondylis V, Pastorino F, Di Paolo D, Perri P, Cossu I, Schorn F, Marinaccio C, Murgia D, and Daga A, et al (2016). A novel liposomal clodronate depletes tumor-associated macrophages in primary and metastatic melanoma: anti-angiogenic and anti-tumor effects. *J Control Release* **223**, 165–177.
- [20] Fritz JM, Tennis MA, Orlicky DJ, Lin H, Ju C, Redente EF, Choo KS, Staab TA, Bouchard RJ, and Merrick DT, et al (2014). Depletion of tumor-associated macrophages slows the growth of chemically induced mouse lung adenocarcinomas. *Front Immunol* **5**, 587.
- [21] Reusser NM, Dalton HJ, Pradeep S, Gonzalez-Villasana V, Jennings NB, Vasquez HG, Wen Y, Rupaimoole R, Nagaraja AS, and Gharpure K, et al (2014). Clodronate inhibits tumor angiogenesis in mouse models of ovarian cancer. *Cancer Biol Ther* **15**, 1061–1067.
- [22] Fleisch H (2002). Development of bisphosphonates. *Breast Cancer Res* **4**, 30–34.
- [23] van Rooijen N and Hendriks E (2010). Liposomes for specific depletion of macrophages from organs and tissues. *Methods Mol Biol* **605**, 189–203.
- [24] Lin HN and O'Connor JP (2017). Osteoclast depletion with clodronate liposomes delays fracture healing in mice. *J Orthop Res* **35**, 1699–1706.
- [25] Diamond P, Labrinidis A, Martin SK, Farrugia AN, Gronthos S, To, L, BFujii N, O'Loughlin PD, Evdokiou A, and Zannettino AC (2009). Targeted disruption of the CXCL12/CXCR4 axis inhibits osteolysis in a murine model of myeloma-associated bone loss. *J Bone Miner Res* **24**, 1150–1161.
- [26] Noll JE, Williams SA, Tong CM, Wang H, Quach JM, Purton LE, Pilkington K, To, L, BEvdokiou A, and Gronthos S, et al (2014). Myeloma plasma cells alter the bone marrow microenvironment by stimulating the proliferation of mesenchymal stromal cells. *Haematologica* **99**, 163–171.
- [27] Cheong CM, Chow AW, Fitter S, Hewett DR, Martin SK, Williams SA, To, L, BZannettino AC, and Vandyke K (2015). Tetraspanin 7 (TSPAN7) expression is upregulated in multiple myeloma patients and inhibits myeloma tumour development in vivo. *Exp Cell Res* **332**, 24–38.
- [28] Noll JE, Hewett DR, Williams SA, Vandyke K, Kok C, To, L, BZannettino AC (2014). SAMS1 is a tumor suppressor gene in multiple myeloma. *Neoplasia* **16**, 572–585.
- [29] Vandyke K, Dewar AL, Diamond P, Fitter S, Schultz CG, Sims NA, and Zannettino AC (2010). The tyrosine kinase inhibitor dasatinib dysregulates bone remodeling through inhibition of osteoclasts in vivo. *J Bone Miner Res* **25**, 1759–1770.
- [30] Mrozik KM, Cheong CM, Hewett D, Chow AW, Blaschuk OW, Zannettino AC, and Vandyke K (2015). Therapeutic targeting of N-cadherin is an effective treatment for multiple myeloma. *Br J Haematol* **171**, 387–399.
- [31] Chow A, Lucas D, Hidalgo A, Mendez-Ferrer S, Hashimoto D, Scheiermann C, Battista M, Leboeuf M, Prophete C, and van Rooijen N, et al (2011). Bone marrow CD169+ macrophages promote the retention of hematopoietic stem and progenitor cells in the mesenchymal stem cell niche. *J Exp Med* **208**, 261–271.
- [32] Winkler IG, Sims NA, Pettit AR, Barbier V, Nowlan B, Helwani F, Poulton IJ, van Rooijen N, Alexander KA, and Raggatt LJ, et al (2010). Bone marrow macrophages maintain hematopoietic stem cell (HSC) niches and their depletion mobilizes HSCs. *Blood* **116**, 4815–4828.
- [33] Croucher P, Jagdev S, and Coleman R (2003). The anti-tumor potential of zoledronic acid. *Breast* **12**(Suppl 2), S30–S36.
- [34] Georgii-Hemming P, Wiklund HJ, Ljunggren O, and Nilsson K (1996). Insulin-like growth factor I is a growth and survival factor in human multiple myeloma cell lines. *Blood* **88**, 2250–2258.
- [35] Qiang YW, Yao L, Tosato G, and Rudikoff S (2004). Insulin-like growth factor I induces migration and invasion of human multiple myeloma cells. *Blood* **103**, 301–308.
- [36] Noll JE, Williams SA, Purton LE, and Zannettino AC (2012). Tug of war in the haematopoietic stem cell niche: do myeloma plasma cells compete for the HSC niche? *Blood Cancer J* **2**, 1–10.
- [37] Moreaux J, Hose D, Kassambara A, Reme T, Moine P, Requirand G, Goldschmidt H, and Klein B (2011). Osteoclast-gene expression profiling reveals osteoclast-derived CCR2 chemokines promoting myeloma cell migration. *Blood* **117**, 1280–1290.
- [38] Wynes MW and Riches DW (2003). Induction of macrophage insulin-like growth factor-I expression by the Th2 cytokines IL-4 and IL-13. *J Immunol* **171**, 3550–3559.
- [39] Short BJ, Brouder N, and Simmons PJ (2009). Prospective isolation of mesenchymal stem cells from mouse compact bone. *Methods Mol Biol* **482**, 259–268.
- [40] Bianco P (2011). Bone and the hematopoietic niche: a tale of two stem cells. *Blood* **117**, 5281–5288.
- [41] Ghobrial IM (2012). Myeloma as a model for the process of metastasis: implications for therapy. *Blood* **120**, 20–30.
- [42] Qian B, Deng Y, Im JH, Muschel RJ, Zou Y, Li J, Lang RA, and Pollard JW (2009). A distinct macrophage population mediates metastatic breast cancer cell extravasation, establishment and growth. *PLoS One* **4**, e6562.
- [43] Schmall A, Al-Tamari HM, Herold S, Kampschulte M, Weigert A, Wietelmann A, Vipotnik N, Grimminger F, Seeger W, and Pullamsetti SS, et al (2015). Macrophage and cancer cell cross-talk via CCR2 and CX3CR1 is a fundamental mechanism driving lung cancer. *Am J Respir Crit Care Med* **191**, 437–447.
- [44] Soki FN, Cho SW, Kim YW, Jones JD, Park SI, Koh AJ, Entezami P, Daigault-Newton S, Pienta KJ, and Roca H, et al (2015). Bone marrow macrophages support prostate cancer growth in bone. *Oncotarget* **6**, 35782–35796.
- [45] Tai YT, Podar K, Catley L, Tseng YH, Akiyama M, Shringarpure R, Burger R, Hideshima T, Chauhan D, and Mitsiades N, et al (2003). Insulin-like growth factor-1 induces adhesion and migration in human multiple myeloma cells via activation of beta1-integrin and phosphatidylinositol 3'-kinase/AKT signaling. *Cancer Res* **63**, 5850–5858.
- [46] Batoon L, Millard SM, Wullschlegel ME, Preda C, Wu AC, Kaur S, Tseng HW, Hume DA, Levesque JP, Raggatt LJ, and Pettit AR (2019). CD169(+) macrophages are critical for osteoblast maintenance and promote intramembranous and endochondral ossification during bone repair. *Biomaterials* **196**, 51–66.
- [47] McCabe A, Zhang Y, Thai V, Jones M, Jordan MB, and MacNamara KC (2015). Macrophage-lineage cells negatively regulate the hematopoietic stem cell pool in response to interferon gamma at steady state and during infection. *Stem Cells* **33**, 2294–2305.
- [48] Crane JL, Zhao L, Frye JS, Xian L, Qiu T, and Cao X (2013). IGF-1 signaling is essential for differentiation of mesenchymal stem cells for peak bone mass. *Bone Res* **1**, 186–194.
- [49] Reagan MR, Liaw L, Rosen CJ, and Ghobrial IM (2015). Dynamic interplay between bone and multiple myeloma: emerging roles of the osteoblast. *Bone* **75**, 161–169.
- [50] Ro TB, Holien T, Fagerli UM, Hov H, Misund K, Waage A, Sundan A, Holt RU, and Borset M (2013). HGF and IGF-1 synergize with SDF-1alpha in promoting migration of myeloma cells by cooperative activation of p21-activated kinase. *Exp Hematol* **41**, 646–655.
- [51] Sugiyama T, Kohara H, Noda M, and Nagasawa T (2006). Maintenance of the hematopoietic stem cell pool by CXCL12-CXCR4 chemokine signaling in bone marrow stromal cell niches. *Immunity* **25**, 977–988.
- [52] Paiva B, Perez-Andres M, Vidrales MB, Almeida J, de las Heras N, Mateos MV, Lopez-Corral L, Gutierrez NC, Blanco J, and Oriol A, et al (2011). Competition between clonal plasma cells and normal cells for potentially overlapping bone marrow niches is associated with a progressively altered cellular distribution in MGUS vs myeloma. *Leukemia* **25**, 697–706.